



Core-level shifts at the Pt/W(1 1 0) monolayer bimetallic interface [☆]

D.M. Riffe ^{a,*}, N.D. Shinn ^b, B. Kim ^{c,d}, K.J. Kim ^e, T.-H. Kang ^d

^a Department of Physics, Utah State University, Logan, UT 84322-4415, USA

^b Sandia National Laboratories, Albuquerque, NM 87185, USA

^c Department of Physics, POSTECH, Pohang, Kyungbuk 790-784, Republic of Korea

^d Beamline Research Division, Pohang Accelerator Laboratory (PAL), Pohang, Kyungbuk 790-784, Republic of Korea

^e Department of Physics, Konkuk University, Seoul 143-701, Republic of Korea

ARTICLE INFO

Article history:

Received 11 July 2009

Accepted for publication 1 October 2009

Available online 14 October 2009

Keywords:

Bimetallic surfaces

Nickel

Palladium

Platinum

Soft X-ray photoelectron spectroscopy

Surface electronic structure

Tungsten

ABSTRACT

We have measured W and Pt 4f_{7/2} core-level photoemission spectra from interfaces formed by ultrathin Pt layers on W(1 1 0), completing our core-level measurements of W(1 1 0)-based bimetallic interfaces involving the group-10 metals Ni, Pd, and Pt. With increasing Pt coverage the sequence of W spectra can be described using three interfacial core-level peaks with binding-energy (BE) shifts (compared to the bulk) of -0.220 ± 0.015 , -0.060 ± 0.015 , and $+0.110 \pm 0.010$ eV. We assign these features to 1D, 2D pseudomorphic (ps), and 2D closed-packed (cp) Pt phases, respectively. For ~ 1 ps ML the Pt 4f_{7/2} BE is 71.40 ± 0.02 eV, a shift of $+0.46 \pm 0.09$ eV with respect to the BE of bulk Pt metal. The W 4f_{7/2} core-level shifts induced by all three adsorbates are semiquantitatively described by the Born–Haber-cycle based partial-shift model of Nilsson et al. [39]. As with Ni/W(1 1 0), the difference in W 4f_{7/2} binding energies between ps and cp Pt phases has a large structural contribution. The Pt 4f lineshape is consistent with a small density of states at the Fermi level, reflective of the Pt monolayer having noble-metal-like electronic structure.

© 2009 Elsevier B.V. All rights reserved.

1. Introduction

The chemical properties of the group-10 metals Ni, Pd, and Pt are strongly correlated with the average energy of their valence *d*bands [1–4]. This is reflected in the interaction of these atoms with simple species such as H₂ and CO [2,5–7] as well as with complex hydrocarbons [1,3]. One method to dramatically alter the *d*bands of Ni, Pd, or Pt (as compared to the surface of the elemental metal) is to create a monolayer (ML) of the metal on an early transition-metal surface such as W(1 1 0). For all three metals the interaction with an early transition-metal substrate substantially lowers the average *d*-band energy, resulting in adlayer electronic structure akin to that of a noble metal [8].

The electronic structure of these adlayers can be directly probed with photoemission spectroscopy. Indeed, monolayer bimetallic interfaces formed by all three group-10 metals on W(1 1 0) have been studied with valence-band (VB) photoemission [9–13], and electronic states associated with the adlayers have been identified

[9–12]. The results are not inconsistent with a negative energy shift of the adlayers' *d*bands. However, owing to the momentum-resolved nature of the VB photoemission measurements, it is non-trivial to obtain a clear picture of the average behavior of the adlayer's *d*band. Indeed, we are aware of only one study of a group-10 metal on an early transition metal [Pd/Nb(1 0 0)] where the *d*-band density of states (DOS) has been estimated from momentum-resolved VB photoemission measurements [14].

The complexity inherent in VB photoemission can be circumvented by measuring core-level shifts of the adlayer atoms, instead, because changes in core-level energies are often nearly equal to changes in the average *d*-band energy [15–17]. Core-level photoemission can thus provide a view of the averaged *d*-band electronic structure at a bimetallic interface. Indeed, X-ray photoelectron spectroscopy (XPS) measurements of monolayer Ni, Pd, and Pt core-level shifts on a variety of substrates reveal a strong correlation between the core-level shifts and the chemical properties of the overlayers [5,6,18].

Core-level photoemission has also been used to probe the substrate atoms at group-10/early-transition-metal interfaces [8,19–23], but except for core-level measurements of W(1 1 1) by Tao et al. [20], none of this work has been particularly systematic. This is unfortunate because the substrate shifts provide a view of the interface that is complementary to the adlayer shifts. Further, as Weinert and Watson have pointed out [16], in comparison with adlayer core-level shifts, substrate shifts may provide a more direct

[☆] This manuscript has been authored by Sandia Corporation under Contract No. DE-AC04-94AL85000 with the US Department of Energy. By accepting the article for publication the publisher acknowledges that the United States Government retains a non-exclusive, paid-up, irrevocable, World-wide license to publish or reproduce the published form of this manuscript, or allow others to do so, for United States Government purposes.

* Corresponding author. Tel.: +1 435 797 3896; fax: +1 435 797 2491.

E-mail address: riffe@cc.usu.edu (D.M. Riffe).

measure of the charge redistribution associated with the bonding between the adlayer and substrate.

In order to systematically assess the interfaces formed by the three group-10 metals on an early transition metal, we have obtained W(1 1 0) $4f_{7/2}$ core-level spectra upon submonolayer to near-monolayer Ni, Pd, and Pt adsorption. The simple core-level structure of the clean W(1 1 0) surface [as compared to W(1 1 1), for example] makes this face of W an ideal substrate for core-level photoemission investigations of interfacial electronic structure. This simplicity has been utilized in a number of previous investigations of W-substrate based bimetallic interfaces [24–34]. Our results for Ni and Pd have recently been reported [35,36]; here we present the Pt induced shifts. In addition to the substrate core-level spectra, we have also obtained $4f$ spectra from the overlayer Pt atoms at a coverage of ~ 1 ML.

Using these new data from Pt/W(1 1 0) and previous data from Ni/W(1 1 0) [35,37] and Pd/W(1 1 0) [36–38], we are able to identify several general features of the core-level spectra from all three systems. First, with respect to the core-level binding energies (BE's) of atoms at their respective clean surfaces, the core-level shifts of both the substrate and overlayer atoms are positive, and [for a pseudomorphic (ps) overlayer] the ratio of the overlayer shift to substrate shift is ~ 4 in all three cases. Second, for the two metals (Ni and Pt) that also form a closed-packed (cp), commensurate phase, only a single substrate core-level feature is associated with this phase, even though the commensurate nature of the overlayer means that not all surface W atoms have the same overlayer-atom coordination. Third, for both Ni/W(1 1 0) and Pt/W(1 1 0) there is a surprisingly large difference in the W core-level BE between the ps and cp phases. This large difference indicates a significant structural contribution to the substrate BE shifts. To gain insight into the substrate shifts we use the partial-shift model of Nilsson and coworkers [39], which semiquantitatively describes both the overall shifts as well as the structural contributions to them.

In addition to these general features we also (i) discuss the substrate core-level shifts in terms of adlayer heats of adsorption, (ii) discuss the relationship of the Pt core-level lineshape to the Pt $5d$ electronic structure, and (iii) compare the substrate shifts induced by the group-10 metals on W(1 1 0) to those at the W(1 1 1) surface.

2. Experimental details

The core-level photoemission spectra were obtained using beamline U16A at the National Synchrotron Light Source, which includes a 6-m toroidal-grating-monochromator and an end station with a 150 mm hemispherical electron-energy analyzer. The W (Pt) core-level spectra were obtained using 92 (112) eV photons at a total (photon plus electron energy) resolution of ~ 100 (~ 250) meV.

The W crystal was cleaned by the standard technique of sample annealing at 1550 K in an oxygen environment with periodic flashes to 2400 K [40]. As discussed in detail below, cleanliness is assessed via W $4f_{7/2}$ photoemission spectra from a freshly flashed sample. We estimate surface contamination to be much less than 1% of a monolayer (ML). The Pt layers were deposited on the room temperature W surface from a shuttered evaporator surrounded by a liquid-nitrogen-cooled shroud. Adsorption rates were on the order of 0.1 ML/min.

3. Results and analysis

The data in Fig. 1 illustrate the progression of the W $4f_{7/2}$ spectrum with increasing Pt deposition. The top curve, from a clean surface, consists of two peaks: the lower binding-energy (BE) peak

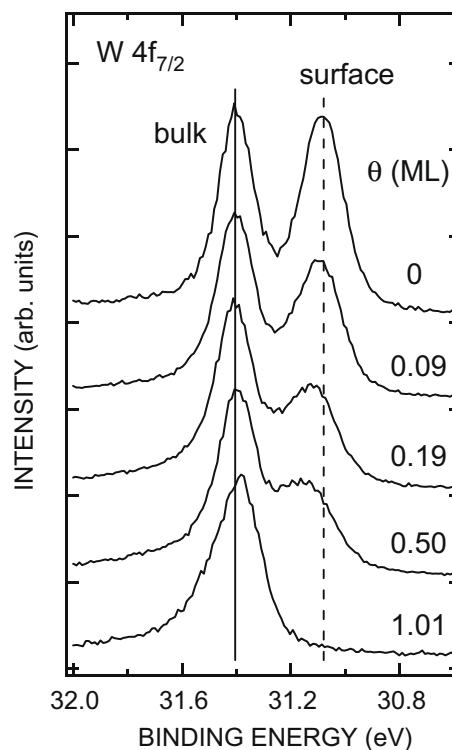


Fig. 1. W $4f_{7/2}$ core-level spectra from the Pt/W(1 1 0) bimetallic interface, illustrating the effect of increasing Pt coverage. The solid and dashed lines mark the positions of the bulk and clean-surface core-level features, respectively.

(surface) is from W atoms in the first atomic layer, and the higher BE peak (bulk) is from W atoms in the second atomic layer and deeper [41,42]. The solid and dashed lines mark the BE's of the bulk and clean-surface atoms, respectively. As in the case of Ni deposition on W(1 1 0) [35], with increasing coverage the surface peak diminishes in height until only one peak is visible. For Pt this single peak is very close to the BE of the bulk peak, suggesting that at higher coverages the Pt influenced atoms have BE's that are close to the bulk-atom BE.

We use least-squares fitting to decompose the core-level data into spectral components. Each core-level photoemission component is modeled by a Gaussian broadened Doniach–Šunjić (DS) peak [42,43], which is described by five parameters: a Lorentzian width, singularity index, binding energy, peak height, and Gaussian width. We use a linear function to describe the background of the W spectra. In fitting the Pt $4f$ spectra, discussed below, the nonlinearity of the background is modeled using a power-law term.

Fig. 2a illustrates a least-squares fit to a W $4f_{7/2}$ spectrum from a clean W(1 1 0) surface before Pt deposition. The fit contains two DS-peaks (labeled B and S) that have parameters consistent with data obtained at slightly higher resolution [42]. That other components are not needed to describe this spectrum indicates that surface contamination is well below 0.01 ML [35].

Because the Pt-induced components of the W $4f_{7/2}$ spectra are not resolved, it is necessary to constrain some of the parameters in order to obtain physically reasonable results from the analysis. First, the B and S Lorentzian widths are held equal to values determined from clean-surface spectra [42]. Second, because the B and S components have nearly identical phonon broadenings [42], their Gaussian widths are constrained to the same (fitted) values. Third, because the interfacial components are from atoms more highly coordinated than the clean-surface atoms, the Lorentzian and Gaussian parameters of these components are constrained to match the B feature. As for the singularity index, which describes

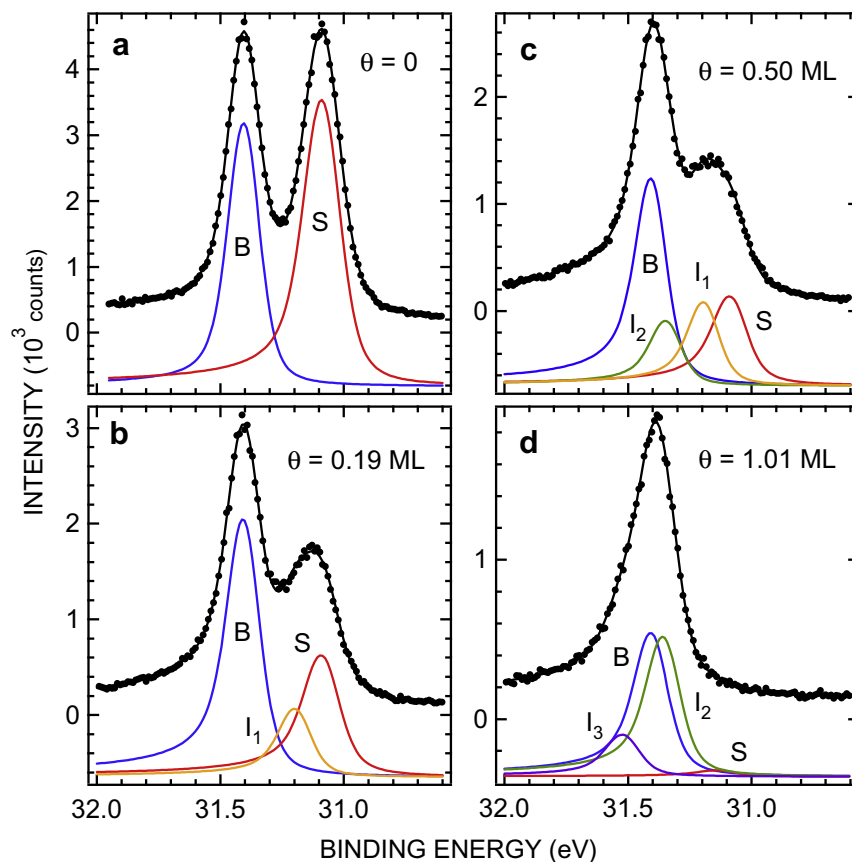


Fig. 2. Least-squares analysis of W $4f_{7/2}$ core-level spectra from the Pt/W(1 1 0) bimetallic interface. Peaks due to bulk W (B), clean surface W (S), and W atoms coordinated by 1D Pt rows (I_1), ps Pt (I_2), and cp Pt (I_3) are shown. Indicated coverages of Pt are in units of a ps ML.

the high-binding energy tail of each component, we find for Pt coverages above ~ 0.2 ML that this parameter must be allowed to increase slightly above values for the B and S atoms in clean-surface spectra.

With these constraints the least-squares analysis provides the following insights into the W $4f_{7/2}$ spectra from the Pt-covered surface. As Fig. 2b–d illustrates, three Pt-induced components are required to model spectra over the range of measured coverages, up to ~ 1 pseudomorphic (ps) ML. At the lowest Pt coverages (Fig. 2b) a single interfacial core-level component (I_1) appears; the I_1 component has an interfacial core-level shift (ICS) of -220 ± 15 meV.¹ With increasing coverage (Fig. 2c) a second interfacial component (I_2) emerges, with an ICS of -60 ± 15 meV. Finally, at the highest coverages in our study (~ 1 ps ML), the I_1 component vanishes, the S component nearly vanishes, but a third interfacial component (I_3) appears, with an ICS of $+110 \pm 10$ meV.

We also obtained Pt $4f$ photoemission data for coverages near 1 ps ML. Fig. 3a shows a Pt $4f_{7/2}$ spectrum and DS fit. A complete $4f$ spectrum and fit with 2 DS peaks are shown in Fig. 3b. In fitting spectra with both $4f_{5/2}$ and $4f_{7/2}$ components we constrain the singularity index and Gaussian width to be the same for both DS peaks, but the Lorentzian widths are independently fit to account for additional Coster-Kronig broadening of the $4f_{5/2}$ component. From the data we determine the following values for the DS parameters: a $4f_{7/2}$ Lorentzian width (FWHM) of 0.41 ± 0.05 eV, a $4f_{5/2}$ Lorentzian width of 0.47 ± 0.06 eV, a singularity index of

0.08 ± 0.03 , and a Gaussian width of 0.35 ± 0.03 eV. A value of 3.35 ± 0.02 eV is determined for the spin-orbit splitting.

From these data we also determine the Pt $4f_{7/2}$ core-level BE. Using the relative kinetic energies of the Pt and bulk-W $4f_{7/2}$ features (35.86 ± 0.01 and 55.85 ± 0.01 eV, respectively), the difference in photon energies (20 eV), and the bulk-W $4f_{7/2}$ BE of 31.41 ± 0.01 eV [44], we obtain a BE of 71.40 ± 0.02 eV for ML Pt/W(1 1 0). Using reported values of the bulk Pt BE [45–58] we ascertain a value of 70.94 ± 0.08 eV for the BE of bulk Pt, yielding a core-level shift of $+0.46 \pm 0.09$ eV for the Pt monolayer. We do not observe any shift in the Pt BE that might be associated with the transformation from the ps to the cp phase.

4. Discussion

4.1. Assignments of spectral components and determination of Pt coverages

Prior structural work on Pt/W(1 1 0) by Kołaczkiwicz and Bauer (KB) [59–63] is key to understanding the origins of the interfacial core-level components illustrated in Fig. 2. Although Pt adsorption in the KB work was typically carried out near 400 K (owing to sample heating by the Pt source), similar structural results obtained by field-ion microscopy (FIM) at lower temperatures indicate that room-temperature adsorption is not significantly different from that at 400 K [64–66]. The KB studies show that initially Pt forms 1D chains oriented along the $\langle 111 \rangle$ directions. With increasing coverage the chains coalesce into 2D ps regions. Finally, above $\theta \approx 0.67$ closed-packed (cp), Nishiyama-Wassermann oriented regions with a local density of 13/11 ML begin to

¹ The interfacial core-level shift is defined as the difference in binding energy between a Pt influenced core-level and the binding energy of bulk W atoms.

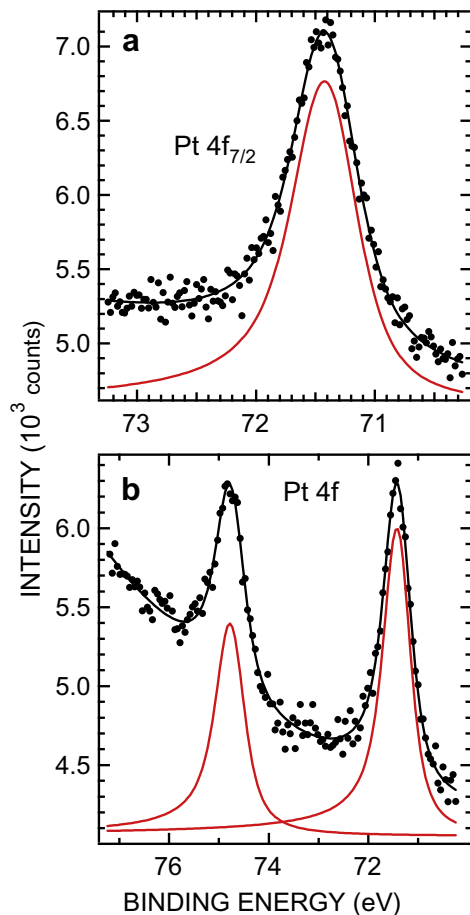


Fig. 3. Least-squares analysis of Pt 4f core-level spectra from the Pt/W(1 1 0) bimetallic interface for ~ 1 ML of Pt.

form. We thus assign the three core-level components I_1 , I_2 , and I_3 to surface W atoms interacting with 1D Pt chains, ps Pt regions, and cp Pt regions, respectively. As discussed in Section 4.3, an increasing shift of the first-layer-atom BE with increasing local Pt coverage is theoretically expected.

With these assignments we can estimate the Pt coverage associated with each spectrum using the relative intensities of the first-layer (S , I_1 , I_2 , and I_3) W core-level components. Assuming that the i th core-level peak is associated with a particular local Pt coverage θ_i , the total Pt coverage θ can be written as the weighted average over all local coverages

$$\theta = \frac{\sum_i \theta_i F_i e^{d_i/\lambda}}{\sum_i F_i e^{d_i/\lambda}}, \quad (1)$$

where the weight function $F_i e^{d_i/\lambda}$ is the product of the integrated intensity F_i of a particular core-level line and a factor $e^{d_i/\lambda}$ that accounts for the attenuation of the intensity due to the Pt overlayer. In this second factor d_i is the thickness of the i th overlayer, and λ is the inelastic mean free path in Ni. We estimate the overlayer thickness from the ratio of the local surface density to the volume density of bulk Pt. For λ we use a value of 0.47 nm [67]. For the clean-surface atoms $\theta_i = 0$, for the 1D Pt chains $\theta_i = 1/2$ ML [60], for the ps-layer-covered atoms $\theta_i = 1$ ML, and for the cp-layer-covered atoms $\theta_i = 13/11$ ML [61]. Eq. (1) is also predicated on insignificant variations in component intensities due to electron diffraction. We point out that we have previously used Eq. (1) to determine Ni coverages on W(1 1 0) [35].

Our combined results for the coverages and spectral assignments are consistent with the structural studies of KB. As a function of coverage KB observe a transition in their low-energy electron diffraction (LEED) pattern at ~ 0.2 ML [61] that can be associated with the beginning of the coalescence of the 1D chains. Consistent with this observation, we observe only the I_1 component for $\theta \lesssim 0.2$ ML. Similarly, the LEED data of KB indicate that cp areas begin to form at $\theta \approx 0.67$ ML [61]. Consistent with this, we do not observe the I_3 feature at 0.5 ML, but only in spectra much closer to 1 ML.

Table 1 summarizes the measured core-level shifts associated with Pt on W(1 1 0). Here we list not only the ICS of each phase, but also the shift of the W $4f_{7/2}$ core-levels with respect to the W(1 1 0) clean-surface BE, which is known as the adhesion core-level shift (ACS) [68], and the shift of the Pt $4f_{7/2}$ core-level with respect to the Pt(1 0 0) surface, which is known as the adlayer core-level shift (AdCS) [69]. This last shift is obtained using a value of -0.56 ± 0.01 eV for the (unreconstructed) Pt(1 0 0) surface core-level shift [56,58].

4.2. General features of group-10-metals/W(1 1 0) core-level shifts

There are features common to the ACS's and AdCS's associated with pseudomorphic monolayers of Ni, Pd, and Pt on W(1 1 0). The first general feature is the relative size of the interfacial shifts for each system. As Table 2 shows, the ACS and AdCS are both positive for each system, and the AdCS is significantly larger than the ACS: on average the AdCS is ~ 4 times larger than the corresponding ACS. These experimental results are consistent with Wu and coworkers' *ab initio* calculated shifts for a ps ML of Ni or Pd on W(1 1 0) [70,71], also summarized in Table 2. The agreement between experiment and theory is especially good for Pd/W(1 1 0).

Results from the theoretical studies of Wu et al. [70,71], which also include an analysis of charge redistribution at the bimetallic interface, imply that the core-level shifts can be qualitatively understood in terms of this redistribution of charge. We first note that the calculated shifts include only initial (ground) state contributions. That is, they do not include differences in the core-hole

Table 1
Experimental core-level shifts at the Pt/W(1 1 0) interface.

Core-level	Pt phase	ICS (meV)	ACS (meV)	AdCS (meV)
W $4f_{7/2}$	1D chains	-220 ± 15	100 ± 15	
	ps ML	-60 ± 15	260 ± 15	
	cp ML	110 ± 10	430 ± 10	
Pt $4f_{7/2}$	ps ML	460 ± 90		1020 ± 90

Table 2
Substrate ACS's and adlayer AdCS's and for pseudomorphic Ni, Pd, and Pt on W(1 1 0). All adlayers AdCS's are with respect to the core-electron BE at the respective (1 0 0) surface.

Adlayer	Substrate ACS (meV)		Adlayer AdCS (meV)		
	Expt.	Theory	Partial shift	Expt.	Theory
Ni	90 ^a	210 ^d	130	400 ^f	540 ^d
Pd	230 ^b	250 ^e	230	800 ^g	830 ^e
Pt	260 ^c		260	1020 ^c	

^a Ref. [35].

^b Ref. [36].

^c This study.

^d Ref. [71].

^e Ref. [70].

^f Ref. [37].

^g Ref. [38].

screening energy in the final (excited) state of the photoemission process. Given the good agreement between the experimental and theoretical shifts, we can thus infer that final-state contributions are secondary for these systems, and so the shifts are mainly due to differences in the initial states of the involved atoms. An analysis of the shifts in terms of charge redistribution suggests, then, that valence charge density moves away from the cores of both the substrate and adlayer atoms at the interface. This interpretation is supported by the charge-density difference plots of Wu et al. [70,71], which show a depletion of charge near the atoms of both the adlayer and first layer of the substrate and a concurrent buildup of charge in the interstitial region between them. However, the relationship of the charge-density plots to the AdCS is not straightforward because the initial overlayer state for the charge-density plot is not equivalent to the initial state used in calculating the AdCS's. For the former the initial overlayer state is a single, unsupported layer in a bcc(1 1 0) configuration (at the substrate spacing), while for the latter the initial overlayer state is the corresponding (1 0 0) surface of the metal. On the other hand the calculated depletion of charge around the surface W atoms can be more confidently associated with the ACS since the initial states for the *ab initio* theory and ACS determination are the same. Related to these observations, the calculations of Weinert and Watson support the view that the substrate core-level shifts, more than those of the adlayer, are indicative of charge rearrangement associated with bonding at the interface [16].

The second general feature associated with these bimetallic interfaces is the observation that the cp, commensurate phases of Ni/W(1 1 0) and Pt/W(1 1 0) exhibit only one core-level binding energy,² as discussed in detail for Ni/W(1 1 0) [35]. Briefly, this result is surprising because the commensurate nature of the overlayer means that not all surface W atoms have identical coordination to the overlayer atoms. As is observed for O/W(1 1 0) [72], we would expect each differently coordinated W atom to exhibit a different core-level BE, which would minimally result in an inhomogeneously broadened spectral feature associated with the cp phase. However, for both Ni and Pt there is no indication that the cp component is broader than the other spectral components. That different BE's are observed for O/W(1 1 0) but not for Ni or Pt adsorption suggests that the different behaviors stem from the nature of the bonding, which is polarized-covalent in the case of O, but metallic for Ni and Pt.

The third general feature of the core-level spectra from these bimetallic interfaces is the unexpectedly large difference in BE's associated with the ps and cp phases. Simple theory (see Section 4.3) predicts the ACS to be proportional to the overlayer coverage. Given the cp to ps coverage ratio of 1.18 and the ps ACS of 260 meV for Pt/W(1 1 0), a cp ACS of 307 meV is predicted. This value is 123 meV less than the measured cp ACS of 430 meV. This result is very similar to our previous result for Ni/W(1 1 0) [35]. In that system the cp to ps coverage ratio of 1.28 along with the ps ACS of 90 meV predicts a cp ACS of 115 meV, which is 135 meV less than the measured cp ACS of 250 meV. As discussed in detail below these unexpected extra shifts can be attributed to structural differences between the ps and cp layers.

4.3. Born–Haber-cycle analysis of the interfacial shifts

A number of Born–Haber-cycle based approaches have been used to describe core-level BE shifts [39,68,73–76]. For bimetallic interfaces the most straightforward is the partial-shift model of Nilsson et al. [39], which we use here to discuss the W 4f_{7/2} interfacial shifts. Under several simplifying assumptions, previously

discussed in detail [35], the ACS of the W core level can be expressed as

$$\Delta \varepsilon_c^{(I,S)}(Z) = c_M^{(I)} \left[E_{\text{sol}}^Z(M) - E_{\text{sol}}^Z(M) - (E_{\text{coh}}^Z - E_{\text{coh}}^Z) \right]. \quad (2)$$

Here $E_{\text{sol}}^Z(M)$ is the solution energy of a Z atom (W, in the present case) in an M-metal host (Ni, Pd, or Pt), and E_{coh}^Z is the cohesive energy of the Z metal. A core-excited (and fully screened) Z atom is designated by Z'. The parameter $c_M^{(I)}$ is the effective concentration of neighboring M atoms surrounding a Z atom at the interface. For a 2D overlayer $c_M^{(I)}$ is expected to be close to 0.2. Eq. (2) reflects the intuitive expectation that the adlayer-induced shift of the surface-peak BE should be proportional to the concentration of M atoms in the overlayer (as long as the energy terms in Eq. (2) are constant). However, as we discuss in detail below, structural contributions to the solution energies invalidate this simple relationship.

We first use Eq. (2) to calculate the ACS for ps monolayers on W(1 1 0). In the calculations we make the equivalent-cores approximation, in which a Z' atom is assumed to be equivalent to a Z + 1 atom (Re, in the present case) [73]. For the cohesive energies E_{coh}^W and $E_{\text{coh}}^{\text{Re}}$ we use experimental values of 8.899 and 8.031 eV, respectively [77]. For the solution energies we follow de Boer and coworkers' analysis [78], in which the solution energy $E_{\text{sol}}^A(B)$ is described by the solution energy of an A atom in the host metal B in the liquid state [$E_{\text{sol}}^A(B)_0$] with solid-state elastic [$E_{\text{sol}}^A(B)_{\text{el}}$] and structural [$E_{\text{sol}}^A(B)_{\text{st}}$] corrections. For $E_{\text{sol}}^A(B)_0$ and $E_{\text{sol}}^A(B)_{\text{el}}$ we use de Boer's semiempirical values [78]. For $E_{\text{sol}}^A(B)_{\text{st}}$ we use the more modern theory of Ruban et al. [79]. We note that Ruban et al. only give structural contributions to solution energies of 4d-metal atoms in other 4d-metal hosts. However, de Boer et al. argue that this contribution is mainly a function of the number of *d* electrons in each metal [78], and so it should not be too inaccurate, in the present case, to use the structural contributions for Mo (Z) and Tc (Z+1) in Pd (M) in calculating $E_{\text{sol}}^Z(M)_{\text{st}}$ and $E_{\text{sol}}^{Z'}(M)_{\text{st}}$ for all three systems. Calculated values for $\Delta E_{\text{sol}}(M) = E_{\text{sol}}^{Z'}(M) - E_{\text{sol}}^Z(M)$, as well as the three individual contributions, are presented in Table 3. The quantity $\Delta E_{\text{sol}}(M)_{\text{st,bcc}}$ in the table is $\Delta E_{\text{sol}}^A(B)_{\text{st}}$ for solution in a bcc host, which is applicable to a ps overlayer. Note that for solution in an fcc (or hcp) host the sign of this term is changed, but its magnitude remains the same [78].

Adhesion core-level shifts calculated from Eq. (2) with $c_M^{(I)} = 0.2$ are reported in Table 2. Overall the agreement between partial-shift calculated and the experimental results is remarkably good, especially for Pd and Pt. One might argue because Ni is significantly smaller than Pd and Pt that $c_M^{(I)}$ should perhaps be less for a ps layer of Ni, which would produce even better agreement between the partial-shift analysis and experiment, but this is perhaps asking too much of the partial-shift model. Nonetheless, as Table 3 shows the significantly smaller ACS for Ni as compared to Pd and Pt can be traced to the more negative values of $\Delta E_{\text{sol}}(M)_0$ and $\Delta E_{\text{sol}}(M)_{\text{el}}$ for Ni as compared to the other two metals.

The unexpected large differences in ACS's between the ps and cp layers of Ni and Pt can also be understood within the framework of the partial-shift model. For both Ni and Pt the structure of the cp layer is a (slightly distorted) hcp layer [10,80]. Thus, there is an extra contribution to the ACS that is approximately equal to

Table 3

Solution energy differences $\Delta E_{\text{sol}}(M) = E_{\text{sol}}^{Z'}(M) - E_{\text{sol}}^Z(M)$ and the liquid metal, elastic, and structural contributions to the differences.

Overlayer metal (M)	$\Delta E_{\text{sol}}(M)_0$ (eV/atom)	$\Delta E_{\text{sol}}(M)_{\text{el}}$ (eV/atom)	$\Delta E_{\text{sol}}(M)_{\text{st,bcc}}$ (eV/atom)	$\Delta E_{\text{sol}}(M)$ (eV/atom)
Ni	0.25	-0.26	-0.22	-0.23
Pd	0.54	-0.02	-0.22	0.30
Pt	0.64	-0.01	-0.22	0.41

² Pd exhibits only pseudomorphic ordering on W(1 1 0).

$c_M^{(1)} \left[\Delta E_{\text{sol}}(\text{M})_{\text{st,fcc}} - \Delta E_{\text{sol}}(\text{M})_{\text{st,bcc}} \right]$, which is equal to 88 meV for $c_M^{(1)} = 0.2$. This is not too far from the experimental values of 123 meV and 135 meV for Ni and Pt, respectively, as discussed above in Section 4.2.

4.4. Relationship of core-level shifts to heats of adsorption

An alternative Born–Haber–cycle analysis shows that for a ps overlayer the ACS is approximately related to heats of adsorption via

$$\Delta \varepsilon_c^{(1,5)}(Z) = E_{\text{ads}}^{\text{M}}(Z) - E_{\text{ads}}^{\text{M}}(Z^*), \quad (3)$$

where $E_{\text{ads}}^{\text{M}}(Z)$ (here defined to be >0) is the heat of adsorption of an M atom on the Z-metal surface [75]. In the equivalent-cores approximation, then, the ACS should be close to the difference in heats of adsorption of a M atom on W(1 1 0) and an equivalent Re surface. However, because W is bcc and Re is hcp, the best comparison that can be done with experimental heats of adsorption is to use $E_{\text{ads}}^{\text{M}}(\text{Re})$ values from the close-packed Re(0 0 0 1) surface.

Heats of adsorption are typically inferred from thermal-desorption measurements. Of the group-10 metals, apparently only Pd thermal-desorption measurements have been carried out on both W(1 1 0) [63,81,82] and Re(0 0 0 1) [83]. From these measurements we estimate the difference in heats of adsorption for ps Pd on W(1 1 0) and Re(0 0 0 1) to be 0.21 ± 0.01 eV (/atom), which is in quite good agreement with the ps-layer ACS of 0.23 ± 0.01 eV [36].

4.5. Pt core-level line shapes

Information regarding the 5d electronic structure of Pt is contained in the lineshape of the Pt 4f spectra. In particular, because the singularity index is associated with screening of the photoinduced core hole, it provides information on electronic states near the Fermi level E_f . Relevant to the current system is an experimental study of Pt–Sn and Pt–Pb alloys with varying concentrations of Pt [84]. At low Pt concentrations ($\sim 5\%$) the Pt 5d states lie almost entirely below E_f , which results in a very small density of states near E_f . This small DOS is responsible for a relatively small singularity index, which is ~ 0.06 . As the Pt concentration is increased, however, the interatomic coupling of the 5d states increases, which broadens and shifts the 5d-band, resulting in an increased DOS at E_f . Versus Pt concentration the singularity index monotonically increases until it reaches the bulk-Pt value of ~ 0.20 [57,84,85].

The substantially reduced coupling of the Pt 5d states in the Pt/W(1 1 0) ML results in a similarly small singularity index. For a ML of Pt on W(1 1 0) the Pt 4f peaks are well described by DS lineshapes with a singularity index of 0.08 ± 0.03 (see Fig. 3). As in the case of the Pt–Sn and Pt–Pb alloys, the small value can be ascribed to the substantially reduced 5d density of states (DOS) near E_f that is due to the negative shift and concomitant narrowing of the 5d-bands (compared to bulk Pt). This shift and narrowing are responsible for the noble-metal character of the Pt monolayer. It is noteworthy that the singularity index of 0.05 for Au [86] is similar to that for Pt in the overlayer and the two dilute alloy systems.

4.6. Comparisons with other Pt/W core-level studies

In a study preliminary to the one reported here Shinn et al. analyzed two Pt/W(1 1 0) spectra, referenced to a spectrum from a clean W(1 1 0) surface [24]. The conclusion from that study was that a ps layer of Pt induces an ICS of +70 meV in the W core-level binding energy, a result that is clearly at odds with the present result of -60 ± 15 meV. Because of this discrepancy we have reassessed the data from that study and have subsequently found a systematic error that resulted in the previous conclusion. The sys-

tematic error was a shift in the electron kinetic-energy (KE) between the clean and Pt-covered-surface data, which resulted in a misidentification (switching) of the B and I₂ peaks in the near-ML spectrum of the previous study. This shift was most likely the result of a small drift in photon energy during the time (5 days) between collection of the clean-surface and Pt-covered-surface data.

Because of this systematic error, we have reanalyzed the Pt/W(1 1 0) data from the previous study. The results of the new analysis are shown in Fig. 4, where we show fits of the previously published data [24] (parts b and c of Fig. 4) along with a fit of another spectrum (taken on the same day) at even lower Pt coverage (part a). (As originally published, these spectra are plotted versus measured electron KE rather than BE). Aside from the presence of a small lower KE peak, which does not change with Pt coverage and can thus be ascribed to contamination (likely C [35]), these spectra comprise the same components as the spectra in the present study. Because of the low Pt coverages associated with the spectra in Fig. 4a and b, they can be used to reliably locate the bulk component. A comparison of these spectra with the spectrum in Fig. 4c shows that the peak due to ps Pt is indeed at a lower BE (higher KE) than the bulk component. The fitted ps-layer ICS of -50 meV for the data in Fig. 4c is consistent with the value of -60 ± 15 meV obtained in the present study.

Interfacial core-level shifts for Ni, Pd, and Pt monolayers on W(1 1 1) have been studied by Tao et al.: the ICS's are -210 , -90 , and ~ -20 meV for Ni, Pd, and Pt monolayers, respectively [20,35,87]. These shifts are quantitatively very similar to those that we have measured on W(1 1 0): -230 , -90 , and -60 meV [35,36]. As we previously discussed regarding Ni layers on these two W surfaces, such close correspondence of the shifts is expected [35].

In their study of W(1 1 1) based bimetallic interfaces, which included not only Ni, Pd, and Pt but also Co, Au, Ag, Cu, and K, Tao et al. noticed a linear correlation between the overlayer heat of adsorption and the interfacial binding energy [20]. Such a correlation was also suggested by Shinn et al. in their study of Fe, Ni, and Pt on W(1 1 0) [24]. As Eq. (3) in Section 4.4 indicates, the ACS is expected to be approximately equal to the difference in the heat of adsorption of a given adsorbate on the Z and Z + 1 metals. The empirical result of Tao et al. then implies that adsorbates with larger heats of adsorption also tend to have larger differences in the heats of adsorption between W and Re, a result which is perhaps not too surprising.

In order to see if the trend that Tao et al. observe for bimetallic interfaces on W(1 1 1) is followed for group-10 metals on W(1 1 0) we have reviewed the thermal-desorption literature for Ni, [88,89], Pd [63,81,82], and Pt [61,63] on W(1 1 0). Bauer and coworkers have deduced heats of adsorption equal to 4.9, 4.1, and 6.2 eV for ps layers of Ni, Pd, and Pt, respectively [63,89]. Given that the respective ACS's are 0.09, 0.23, and 0.26 eV, the correlation is negligible. However, deduced heats of adsorption depend on a frequency factor ν (also extracted in the Bauer analysis), which is typically between 10^{13} and 10^{17} s⁻¹. Somewhat puzzling is the frequency-factor exponent $\log(\nu) = 13.2$ for Pd versus values of 16.2 and 15.2 for Ni and Pt, respectively. If we suppose, instead, that ν is the same for all three adsorbates, then (using $\log(\nu) = 15$, for example) the thermal-desorption data are consistent with heat-of-adsorption values of 4.6, 4.7, and 6.2 eV for the three group-10 metals.³ While this significantly improves the correlation, it is not nearly as strong as that reported by Tao et al. for the same three metals on W(1 1 1) [20].

³ We estimate the heats of adsorption via $E_{\text{ads}} = RT_p [\ln(T_p \nu_n \sigma^{n-1} / \beta) - \ln(E_{\text{ads}} / RT_p)]$, which is derived under the assumptions that ν and E_{ads} are constant (for a given initial coverage σ). Here R is the gas constant, T_p is the temperature of the peak in the thermal desorption spectrum, β is the heating rate, and n is the order of the desorption process. The quantity $\nu_n \sigma^{n-1}$ is equal to the frequency factor ν .

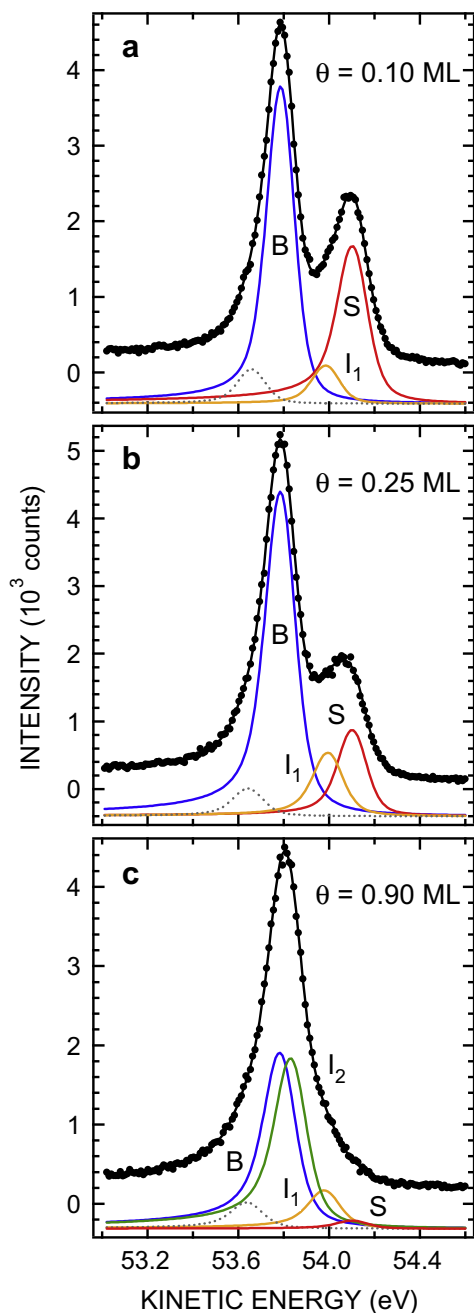


Fig. 4. Least-squares analysis of W $4f_{7/2}$ core-level spectra from an earlier study by Shinn et al. [24]. Note that the spectra are plotted versus electron kinetic energy rather than core-level binding energy.

5. Summary and conclusions

The results presented here complete our study of core-level shifts at the W(1 1 0) surface induced by group-10 metals at sub-monolayer to monolayer coverages. Commonalities among the three bimetallic interfaces include the following: (i) a separate substrate core-level shift can be identified with each overlayer phase; (ii) commensurate overlayers produce only one substrate core-level shift, even though not all substrate atoms are equivalently coordinated; (iii) the difference in substrate shifts induced by pseudomorphic and commensurate overlayers contains a large structural contribution; (iv) for a pseudomorphic overlayer the ratio of adlayer to substrate core-level shifts (when referenced to binding energies at the respective clean surfaces) is ~ 4 for all three

systems; (v) the partial-shift Born–Haber-cycle analysis [39] semi-quantitatively describes the substrate shifts induced by both the pseudomorphic and commensurate layers; and (vi) the corresponding interfacial core-level shifts on W(1 1 0) are very similar to those induced on W(1 1 1).

Interpreting the substrate core-level shifts in terms of charge rearrangement at the bimetallic interfaces, which is supported by the calculations of Wu and coworkers [70,71] and Weinert and Watson [16], suggests that the intermetallic bonding produces a movement of valence charge away from the W surface-atom cores. While not so straightforwardly interpreted, the positive shifts of the overlayer atoms suggest that valence charge also moves away from the adlayer atoms. Taken together the substrate and adlayer shifts imply a buildup of valence charge between the substrate and adlayer atoms. We note that this interpretation of the core-level shifts is consistent with Ruckman and Strongin's interpretation of shifts at the Pd/Ta(1 1 0) interface [8].

In addition to the shifts, the singularity index of the Pt $4f$ features provides insight into the overlayer electronic structure. The significantly smaller value of the singularity index (compared to bulk Pt metal) can be associated with a smaller Pt $5d$ density of states near the Fermi level, as has been previously observed in dilute Pt alloys [84]. The smaller density of states near the Fermi level is a characteristic of the noble-metal-like electronic structure of a group-10-metal monolayer on an early transition-metal surface such as W(1 1 0).

Acknowledgements

This work was supported, in part, by the US Department of Energy, Office of Basic Energy Sciences. Sandia National Laboratories is a multi-program laboratory operated by Sandia Corporation, a Lockheed-Martin Company, for the US Department of Energy under Contract No. DE-AC04-94AL85000. We thank Gunther K. Wertheim for supplying the software program that is used in least-squares fitting of the core-level data.

References

- [1] B. Hammer, J.K. Nørskov, *Adv. Catal.* 45 (2000) 71.
- [2] J.R. Kitchin, J.K. Nørskov, M.A. Barteau, J.G. Chen, *Phys. Rev. Lett.* 93 (2004) 156801.
- [3] J.G. Chen, C.A. Menning, M.B. Zellner, *Surf. Sci. Rep.* 63 (2008) 201.
- [4] J.K. Nørskov, T. Bligaard, J. Rossmeisl, C.H. Christensen, *Nat. Chem.* 1 (2009) 37.
- [5] J. Rodriguez, *Surf. Sci.* 345 (1996) 347.
- [6] B. Hammer, Y. Morikawa, J.K. Nørskov, *Phys. Rev. Lett.* 76 (1996) 2141.
- [7] J.R. Kitchin, J.K. Nørskov, M.A. Barteau, J.G. Chen, *J. Chem. Phys.* 120 (2004) 10240.
- [8] M.W. Ruckman, M. Strongin, *Accounts Chem. Res.* 27 (1994) 250.
- [9] K.-P. Kämper, W. Schmitt, G. Güntherodt, H. Kuhlbeck, *Phys. Rev. B* 38 (1988) 9451.
- [10] C. Koziol, G. Lilienkamp, E. Bauer, *Phys. Rev. B* 41 (1990) 3364.
- [11] G.W. Graham, *J. Vac. Sci. Technol. A* 4 (1986) 760.
- [12] H. Knoppe, E. Bauer, *Zeitschrift für Physikalische Chemie* 202 (1997) 45.
- [13] T.E. Madey, K.-J. Song, C.-Z. Dong, R.A. Demmin, *Surf. Sci.* 247 (1991) 175.
- [14] E. Hüger, K. Osuch, *Phys. Rev. B* 72 (2005) 085432.
- [15] P.H. Citrin, G.K. Wertheim, *Phys. Rev. B* 27 (1983) 3176.
- [16] M. Weinert, R.E. Watson, *Phys. Rev. B* 51 (1995) 17168.
- [17] M.V. Ganduglia-Pirovano, V. Natoli, M.H. Cohen, J. Kudrnovský, I. Turek, *Phys. Rev. B* 54 (1996) 8892.
- [18] J.A. Rodriguez, D.W. Goodman, *Science* 257 (1992) 897.
- [19] M.W. Ruckman, M. Strongin, *Phys. Rev. B* 35 (1987) 487.
- [20] H.-S. Tao, J.E. Rowe, T.E. Madey, *Surf. Sci.* 407 (1998) L640.
- [21] B.S. Mun, C. Lee, V. Stamenkovic, N.M. Markovic, J. Philip, N. Ross, *Phys. Rev. B* 71 (2005) 115420.
- [22] T.H. Andersen, Z. Li, S.V. Hoffmann, L. Bech, J. Onsgaard, *J. Phys.: Condens. Matter* 14 (2002) 7853.
- [23] T. Marten, O. Hellman, A.V. Ruban, W. Olovsson, C. Kramer, J.P. Godowski, L. Bech, Z. Li, J. Onsgaard, I.A. Abrikosov, *Phys. Rev. B* 77 (2008) 125406.
- [24] N.D. Shinn, B. Kim, A.B. Andrews, J.L. Erskine, K.J. Kim, T.-H. Kang, *Mater. Res. Soc. Symp. Proc.* 307 (1993) 167.
- [25] N.D. Shinn, C.H.F. Peden, K.L. Tsang, P.J. Berlowitz, *Phys. Scr.* 41 (1990) 607.
- [26] D.M. Riffe, G.K. Wertheim, P.H. Citrin, *Phys. Rev. Lett.* 64 (1990) 571.

- [27] N.T. Barrett, B. Villette, A. Senhaji, C. Guillot, R. Belkhou, G. Tréglia, B. Legrand, Surf. Sci. 286 (1993) 150.
- [28] G.K. Wertheim, D.M. Riffe, P.H. Citrin, Phys. Rev. B 49 (1994) 4834.
- [29] A.B. Andrews, D.M. Riffe, G.K. Wertheim, Phys. Rev. B 49 (1994) 8396.
- [30] B. Kim, N.D. Shinn, J.L. Erskine, J. Korean Phys. Soc. 30 (1997) 625.
- [31] E.D. Tober, R.X. Ynzunza, F.J. Palomares, Z. Wang, Z. Hussain, M.A. Van Hove, C.S. Fadley, Phys. Rev. Lett. 79 (1997) 2085.
- [32] T.-W. Pi, I.-H. Hong, C.-P. Cheng, Phys. Rev. B 58 (1998) 4149.
- [33] N.P. Tucker, R.I.R. Blyth, R.G. White, M.H. Lee, C. Searle, S.D. Barrett, J. Phys.: Condens. Matter 10 (1998) 6677.
- [34] A.J. Jaworowski, A. Sandell, Surf. Sci. 477 (2001) 141.
- [35] D.M. Riffe, R.T. Franckowiak, N.D. Shinn, B. Kim, K.J. Kim, T.-H. Kang, Surf. Sci. 602 (2008) 2039.
- [36] D.M. Riffe, N.D. Shinn, B. Kim, K.J. Kim, T.-H. Kang, Surf. Sci. 603 (2009) 1070.
- [37] R.A. Campbell, J.A. Rodriguez, D.W. Goodman, Surf. Sci. 240 (1990) 71.
- [38] J.A. Rodriguez, R.A. Campbell, D.W. Goodman, J. Vac. Sci. Technol. A 9 (1991) 1698.
- [39] A. Nilsson, B. Eriksson, N. Mårtensson, J.N. Andersen, J. Onsgaard, Phys. Rev. B 38 (1988) 10357.
- [40] R.G. Musket, W. McLean, C.A. Colmenares, D.M. Makowiecki, W.J. Siekhaus, Appl. Surf. Sci. 10 (1982) 143.
- [41] T.M. Duc, C. Guillot, Y. Lassailly, J. Lecante, Y. Jugnet, J.C. Vedrine, Phys. Rev. Lett. 43 (1979) 789.
- [42] D.M. Riffe, G.K. Wertheim, P.H. Citrin, Phys. Rev. Lett. 63 (1989) 1976.
- [43] S. Doniach, M. Šunjić, J. Phys. C: Solid State Phys. 34 (1970) 285.
- [44] D.M. Riffe, G.K. Wertheim, unpublished.
- [45] R.C. Baetzold, G. Apai, E. Shustorovich, R. Jaeger, Phys. Rev. B 26 (1982) 4022.
- [46] K. Dücker, H.P. Bonzel, Surf. Sci. 213 (1989) 25.
- [47] M. Han, P. Mrozek, A. Wieckowski, Phys. Rev. B 48 (1993) 8329. LP.
- [48] O. Björneholm, A. Nilsson, H. Tillborg, P. Bennich, A. Sandell, B. Hernnäs, C. Puglia, N. Mårtensson, Surf. Sci. 315 (1994) L983.
- [49] E. Janin, M. Björkqvist, T.M. Grehk, M. Göthelid, C.-M. Pradier, U.O. Karlsson, A. Rosengren, Appl. Surf. Sci. 99 (1996) 371.
- [50] S. Ringler, E. Janin, M. Boutonnet-Kizling, M. Göthelid, Appl. Surf. Sci. 162–163 (2000) 190.
- [51] E. Janin, S. Ringler, J. Weissenrieder, T. Åkermark, U.O. Karlsson, M. Göthelid, D. Nordlund, H. Ogasawara, Surf. Sci. 482–485 (2001) 83.
- [52] D. Radosavkic, N. Barrett, R. Belkhou, N. Marsot, C. Guillot, Surf. Sci. 516 (2002) 56.
- [53] H. Ogasawara, B. Brena, D. Nordlund, M. Nyberg, A. Pelmenchikov, L.G.M. Pettersson, A. Nilsson, Phys. Rev. Lett. 89 (2002) 276102.
- [54] J.G. Wang, W.X. Li, M. Borg, J. Gustafson, A. Mikkelsen, T.M. Pedersen, E. Lundgren, J. Weissenrieder, J. Klikovits, M. Schmid, B. Hammer, J.N. Andersen, Phys. Rev. Lett. 95 (2005) 256102.
- [55] B.S. Mun, C. Lee, V. Stamenkovic, N.M. Markovic, J. Ross, N. Philip, J. Chem. Phys. 122 (2005) 184712.
- [56] A. Baraldi, E. Vesselli, L. Bianchettin, G. Comelli, S. Lizzit, L. Petaccia, S. de Gironcoli, A. Locatelli, T.O. Montes, L. Aballe, J. Weissenrieder, J.N. Andersen, J. Chem. Phys. 127 (2007) 164702.
- [57] L. Bianchettin, A. Baraldi, S. de Gironcoli, E. Vesselli, S. Lizzit, L. Petaccia, G. Comelli, R. Rosei, J. Chem. Phys. 128 (2008) 114706.
- [58] A. Baraldi, J. Phys.: Condens. Matter 20 (2008) 093001.
- [59] J. Kolaczkiwicz, E. Bauer, Surf. Sci. 256 (1991) 87.
- [60] J. Kolaczkiwicz, E. Bauer, Phys. Rev. B 44 (1991) 5779.
- [61] J. Kolaczkiwicz, E. Bauer, Surf. Sci. 314 (1994) 221.
- [62] J. Kolaczkiwicz, E. Bauer, Surf. Sci. 366 (1996) 71.
- [63] J. Kolaczkiwicz, E. Bauer, Surf. Sci. 374 (1997) 95.
- [64] D.R. Tice, D.W. Basset, Thin Solid Films 20 (1974) S37.
- [65] D.W. Bassett, J. Phys. C: Solid State Phys. 9 (1976) 2491.
- [66] D.W. Bassett, Thin Solid Films 48 (1978) 237.
- [67] S. Tanuma, C.J. Powell, D.R. Penn, Surf. Interface Anal. 17 (1991) 911.
- [68] N. Mårtensson, A. Stenberg, O. Björneholm, A. Nilsson, J.N. Andersen, Phys. Rev. Lett. 60 (1988) 1731.
- [69] D. Hennig, M.V. Ganduglia-Pirovano, M. Scheffler, Phys. Rev. B 53 (1996) 10344.
- [70] R. Wu, R.R. Freeman, Phys. Rev. B 52 (1995) 12419.
- [71] Z. Yang, R. Wu, Surf. Sci. 469 (2000) 36.
- [72] D.M. Riffe, G.K. Wertheim, Surf. Sci. 399 (1998) 248.
- [73] B. Johansson, N. Mårtensson, Phys. Rev. B 21 (1980) 4427.
- [74] B. Johansson, N. Mårtensson, Helv. Phys. Acta 56 (1983) 405.
- [75] D. Spanjaard, C. Guillot, M.C. Desjonquères, G. Tréglia, J. Lecante, Surf. Sci. Rep. 5 (1985) 1.
- [76] M. Said, M.C. Desjonquères, D. Spanjaard, Surf. Sci. 287/288 (1993) 780.
- [77] C. Kittel, Solid State Physics, Wiley, New York, 2005.
- [78] F.R. de Boer, R. Boom, W.C. M. Mattens, A.R. Miedema, A.K. Niessen, Cohesion in Metals: Transition Metal Alloys, North-Holland, New York, 1988.
- [79] A.V. Ruban, H.L. Skriver, J.K. Nørskov, Phys. Rev. Lett. 80 (1998) 1240.
- [80] J. Kolaczkiwicz, E. Bauer, Surf. Sci. 144 (1984) 495.
- [81] P.J. Berlowitz, D.W. Goodman, Langmuir 4 (1988) 1091.
- [82] W. Schlenk, E. Bauer, Surf. Sci. 93 (1980) 9.
- [83] J.A. Rodriguez, C.T. Campbell, D.W. Goodman, J. Vac. Sci. Technol. A 10 (1992) 2540.
- [84] T.T.P. Cheung, Surf. Sci. 177 (1986) 493.
- [85] S. Hüfner, G.K. Wertheim, Phys. Rev. B 11 (1975) 678.
- [86] P.H. Citrin, G.K. Wertheim, Y. Baer, Phys. Rev. B 27 (1983) 3160.
- [87] H.-S. Tao, C.H. Nien, T.E. Madey, J.E. Rowe, G.K. Wertheim, Surf. Sci. 357/358 (1996) 55.
- [88] P.J. Berlowitz, D.W. Goodman, Surf. Sci. 187 (1987) 463.
- [89] J. Kolaczkiwicz, E. Bauer, Surf. Sci. 175 (1986) 508.